The Osseointegration Properties of Titanium Implants with Hydroxyapatite Submicron-Scale Features in the Rabbit Tibia

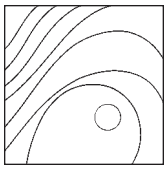

Young-Taeg Sul, DDS, PhD[1]
Ross Towse, BS ChE, MBA[2]

The objective of this study was to biomechanically and histologically assess the stability and integration of titanium implants that include hydroxyapatite based submicron-scale features. Thirty-four 3.4 mm × 6.5 mm implants, equally split between test (grit blasted, etched, and submicron scale deposition) and control (grit blasted and etched) groups, were placed in the tibiae of New Zealand White rabbits. At 3-weeks follow-up, the group with the submicron deposition showed significantly improved bone response compared with the control group. The test group required higher removal torque values, with its post-torque histology demonstrating both enhanced bone formation and an intact interface indicative of a robust bone-to-implant bond. (Int J Periodontics Restorative Dent 2013;33:e18–e25. doi: 10.11607/prd.1685)

[1]Associate Professor, Department of Prosthodontics/Dental Materials Science, Institute of Odontology, The Sahlgrenska Academy, University of Gothenburg, Gothenburg, Sweden.
[2]Director of Research, Biomet 3i, Palm Beach Gardens, Florida.

Correspondence to: Dr Young-Taeg Sul, Department of Prosthodontics/Dental Materials Science, Institute of Odontology, The Sahlgrenska Academy, University of Gothenburg, PO Box 450, SE 405 30 Gothenburg, Sweden; email: young-taeg.sul@biomaterials.gu.se.

Dental implant therapies continue to evolve as patients and subsequently clinicians push for reduced treatment times without compromising performance. The clinical community and implant manufacturers have responded to these needs by providing implant systems with advanced surface technologies intended to enhance osteoconduction mechanisms and the physical and/or biochemic interlocking of de novo bone with the surface.

Regarding these surface technologies, chemical and/or topographic enhancements are now commonplace in implant dentistry. However, chemistry and topography play different but potentially complementary roles in establishing the rate and strength of osseointegration.[1]

Chemistry additions to the implant's titanium oxide surface, including the introduction of ions such as calcium, phosphate, sulfur, and magnesium, have been theorized to create a biochemic bond between the bone tissues and implant interface.[2–5] Evidence of such biochemic bonding includes preclinical studies where titanium

Fig 1 *Commercially pure titanium implant design.*

Table 1 Surface chemistry and topographic levels*

Group	Coarse micron (10+ micron)	Micron (1 to 3 micron)	Submicron (10 to 100 nm)
Control (blast and acid etch)	X	X	Not present
Test (blast, acid etch, and hydroxyapatite DCD)	X	X	X

*In this experiment, the independent variable evaluated was the addition of a submicron topography and its chemistry.

implants with equivalent roughness were evaluated with the independent variable of surface chemistry. These studies resulted in statistically higher biomechanic force outcomes for implants with metal cation– or anion-enhanced titanium oxide chemistries.[6–8]

Micron-level topographies, created through technologies such as grit blasting and/or acid etching, are also included on many modern implant designs. These modifications have been shown to influence osteoconduction mechanisms, including clot retention and platelet interactions.[9–11] Additionally, the micron-scale topographic features provide undercuts and void volume for the physical interlocking with de novo bone.[12] Numerous preclinical studies have shown the potential biomechanic advantages of micron-level topographies.[13–15]

The most recent trend in implant surface design is the addition of submicron-scale features (eg, 10 to 100 nanometers). Submicron-scale features have been theorized to influence protein absorption and the subsequent mechanisms of osteoconduction.[16] When these features are created using hydroxyapatite or cation/anion-enhanced chemistries, the potential for both a biochemic bond and topographic interlock is also possible. Preclinical research has shown that minimally rough[17] (Sa: mean absolute height deviation < 1 micron) dual acid-etched implants, which include the independent variable of a deposition of discrete crystals of submicron-scale hydroxyapatite, demonstrate both increased osteoconduction and biomechanic strength in early healing.[18–20]

This study builds upon this research base, subsequently exploring the histologic and biomechanic impacts of a hydroxyapatite-based submicron-scale enhancement included on moderately rough[17] (1 micron ≤ Sa ≤ 2 microns) grit-blasted and acid-etched surfaces.

Method and materials

Implant design and surface characteristics

Two groups of experimental screw-shaped commercially pure titanium implants (Biomet 3i) were used in this study. The implants shared the same 3.4-mm-wide × 6.5-mm-long parallel wall design with an external hex connection (Fig 1).

Both the control and test groups had a dual level surface topography created through grit blasting with calcium phosphate–based resorbable blast media, followed by acid etching (BAE). The test group was processed further through a colloidal discrete crystal deposition (DCD) process. The colloid was composed of an alcohol and ≥ 95% crystalline and phase pure hydroxyapatite ($Ca_{10}(PO_4)_6(OH)_2$). The DCD process adhered submicron-scale hydroxyapatite crystals to approximately 50% of the surface (BAE + DCD), thus creating a third level of chemical and topographic features (Table 1) on the test group only.

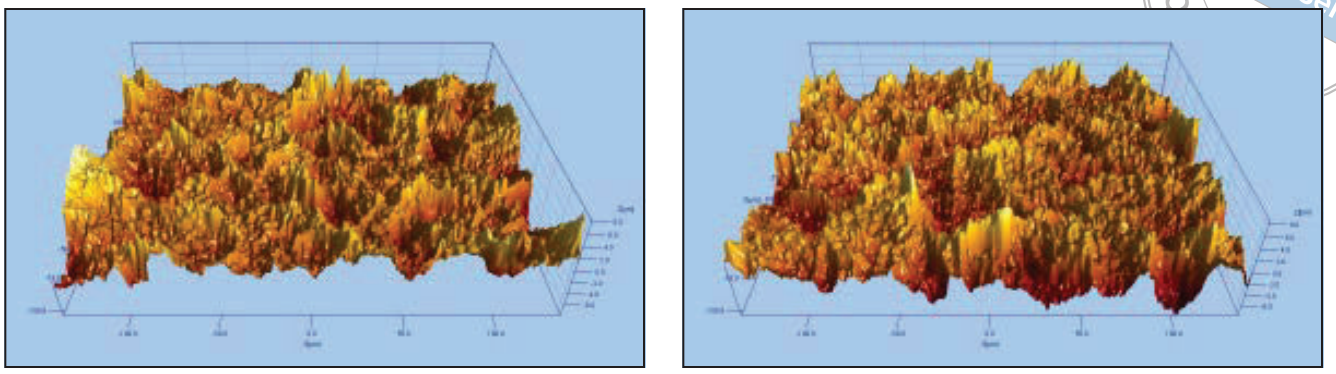

Fig 2 *At low magnification, both the test and control groups demonstrated similar coarse micron attributes and surface characterization parameters (original magnification ×312).*

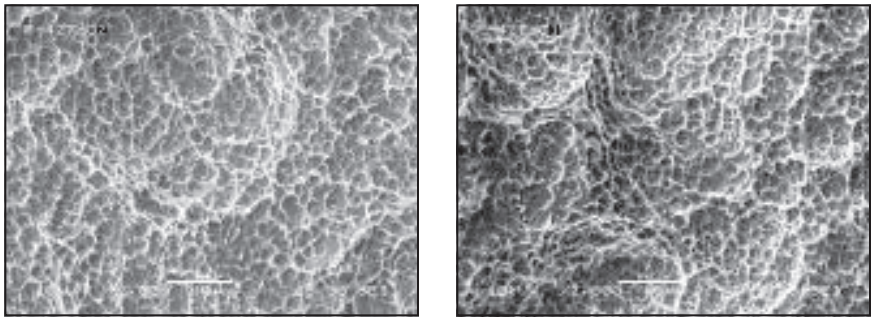

Fig 3 *At high magnification, both test and control groups demonstrated similar micron topography, including 1- to 3-micron peak-to-peak pits (original magnification ×2,000).*

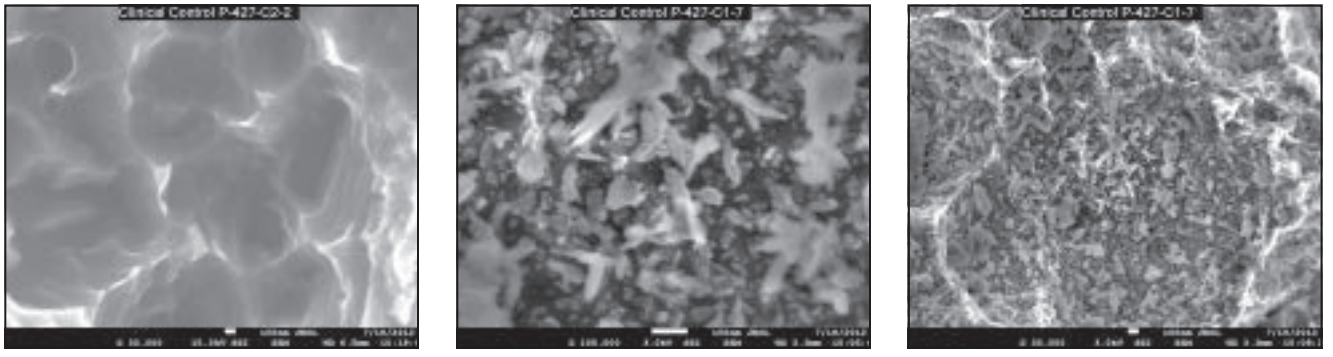

Fig 4 *At very high magnification, the control group surface was relatively devoid of submicron-scale features while the test group demonstrated a complex submicron topography (original magnification ×30,000 and ×100,000).*

The implant surfaces were evaluated using four different methodologies to characterize their complexity. A light interferometer (Micro XAM, ADE Phase Shift) was used for coarse micron surface analysis (Fig 2). The images and data were obtained at ×312.5 magnification (52,400-μm^2 area), using postprocessing, including a 50-μm Gaussian filter and inverse fast Fourier transformation.

Scanning electron microscopy, employing standard and field emission technologies (JEOL JSM-6460LV and JSM-7500F), was used to qualitatively characterize the micron- and submicron-scale features. The micron topography was assessed at ×2,000 magnification (Fig 3), while the submicron-scale features were assessed at ×30,000 and ×100,000 magnification as applicable (Fig 4).

Electron dispersive spectroscopy (JEOL JSM-6460LV with Oxford Instruments INCA EDX) was used to characterize the surface chemistry of the implants (Table 2). This type of analysis is semiquantitative, providing the chemical make-up of approximately 1 to 2 microns of surface depth.[21]

Table 2 **Electron dispersion spectroscopy of surface chemistry (atomic %)**

Group	Carbon	Oxygen	Calcium	Phosphorous	Titanium
Control (blast and acid etch)	3.1	Not detected	Not detected	Not detected	96.9
Test* (blast, acid etch, and hydroxyapatite DCD)	4.2	27.9	1.0	0.8	66.1

*The test group demonstrated small percentages of calcium and phosphorous from the hydroxyapatite deposition.

Animals and surgical technique

Mature New Zealand White rabbits were used in this study, which was approved by the local animal ethics committee at the University of Gothenburg, Sweden. Their mean weight was about 4.3 kg. Three implants were placed into two tibiae of each rabbit. A predetermined randomization pattern was used. For surgery, the animals were anesthetized with intramuscular injections of fentanyl and fluanisone (Hypnorm Vet, Janssen) at 0.5 mL/kg body weight and intraperitoneal injections of diazepam (Valium, Roche) at 2.5 mg/animal. The skin and fascial layers were opened and closed separately. The periosteal layer was gently pulled away from the surgical area and was not sutured. First, point drills were used to create pilot holes for the implants, followed by twist drills of 2.0-mm diameter, 2.0/2.75-mm diameter, and 3.0-mm diameter. Premounted implants were placed using the drill unit handpiece. The mounts were removed, applicable resonance frequency testing was conducted, and the site was closed for healing. The animals were housed individually and were allowed full weight bearing immediately after surgery.

Sacrifice timepoint

The animals were sacrificed after 3 weeks of healing. Based upon the well-accepted contact osteogenesis theory,[9] it was anticipated that new bone formation would initiate at the implant surface expanding and maturing outward. Therefore, the initial de novo bone-to-implant bond was expected to be chemical, followed by a mechanical interlocking with each successive scale of available topography and ultimately with the macro geometric features of the implant. Subsequently, an early healing timepoint was selected to best isolate the biomechanic impacts of the independent variable of a hydroxyapatite chemistry–based, submicron topography enhancement. If a longer healing timepoint was selected, it was hypothesized that the eventual bone interlocking with the coarser micron-scale features and threads would overwhelm the independent variable's impact, disguising its biomechanic strength contributions during the critical, early healing phase.

Resonance fequency and removal torque measurements

Implant stability was measured using a resonance frequency analyzer (Osstell, Integration Diagnostics) at the time of implant placement and 3 weeks postplacement. The resonance frequency analysis (RFA) values reported are a mean of four measurements from each implant, ie, twice at two directions of the transducer parallel and perpendicular to the long axis of the tibia (Fig 5a). After 3 weeks of follow-up, the animals were sacrificed by intravenous injections of pentobarbitalum (Apoteksbolaget). The peak removal torque (RTQ) values of the

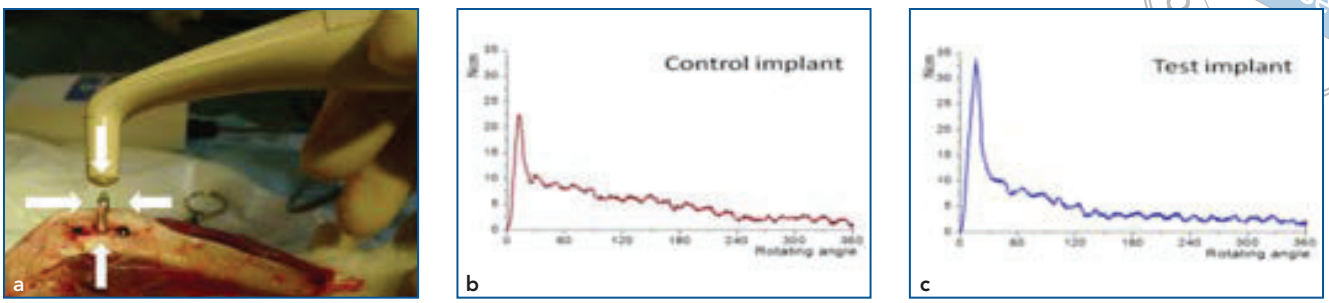

Fig 5 *RFA values were obtained by four measurements, ie, twice at two directions of the transducer parallel and perpendicular to the long axis of the tibia* (a). *Characteristic curves of removal torque show representative values of* (b) *control and* (c) *test groups. One complete rotation is measured as a 360-degree counterclockwise angle.*

Table 3 **Resonance frequency analysis values**

Group*	Mean ISQ values at surgery (SD)	Mean ISQ values at 3 weeks (SD)
Control (blast and acid etch)	57.73 (12.82)	75.58 (6.47)
Test (blast, acid etch, and hydroxyapatite DCD)	57.87 (9.87)	77.75 (3.07)

ISQ = implant stability quotient.
*Both groups demonstrated similar surgical and posthealing results.

implants in bone were measured using a newly developed system that is highly filtered to measure the small changes in the torque value. The tester is controlled by a personal computer that monitors a graphic measurement of torque value and allows a three-dimensional adjustment of the rotation axis along the transducer and the implant at the micrometer scale. The peak RTQ values obtained are determined from a graphic plot of RTQ value, Ncm versus rotation angle (Figs 5b and 5c). In contrast to previous manual test methods, the present automated measuring system provides increased repeatability and reproducibility by minimizing the operator dependency variable.

Histologic observations

After RFA and RTQ measurement, the same samples were prepared for undecalcified cut and ground sections by using the Exakt system.[22,23] The sections were ground to a final thickness of approximately 20 to 30 microns and stained with toluidine blue and 1% pyronin G. The formation of new bone was quantified using a Nikon Eclipse Ci-L microscope coupled to an Easy Image 2000 system (Teknoptik) with ×10 (numerical apperture [NA] 0.30) and ×40 (NA 0.70) objective lenses and a ×10 eyepiece. Measurement of new bone formation on the implant surface after RFA and RTQ testing has been validated for evaluating osteoconductivity of the implant.[5,24] Newly formed bone was quantified around all inside threads of the implants, including periosteal bone formation, endosteal bone formation (inside the threads against the old cortical bone), and endosteal downgrowth (below the old cortex).[24]

Statistical analysis

The statistics program SPSS version 16 (SPSS, IBM) was used for all statistical analyses. Differences were considered as highly statistically significant when $P \leq .01$, statistically significant when $P \leq .05$, and not significant when $P > .05$. The means of RFA, RTQ, and newly formed bone of the groups were compared using nonparametric, Wilcoxin signed rank testing.

Results

RFA measurements

There were no significant differences in mean ISQ values between the test and control groups at both surgery and sacrifice ($P > .05$) (Table 3).

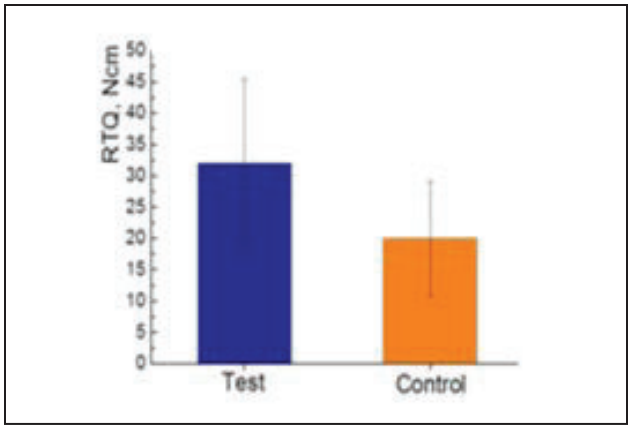

Fig 6 *Mean peak RTQ values after 3 weeks of healing. The test group demonstrated significantly higher RTQ values.*

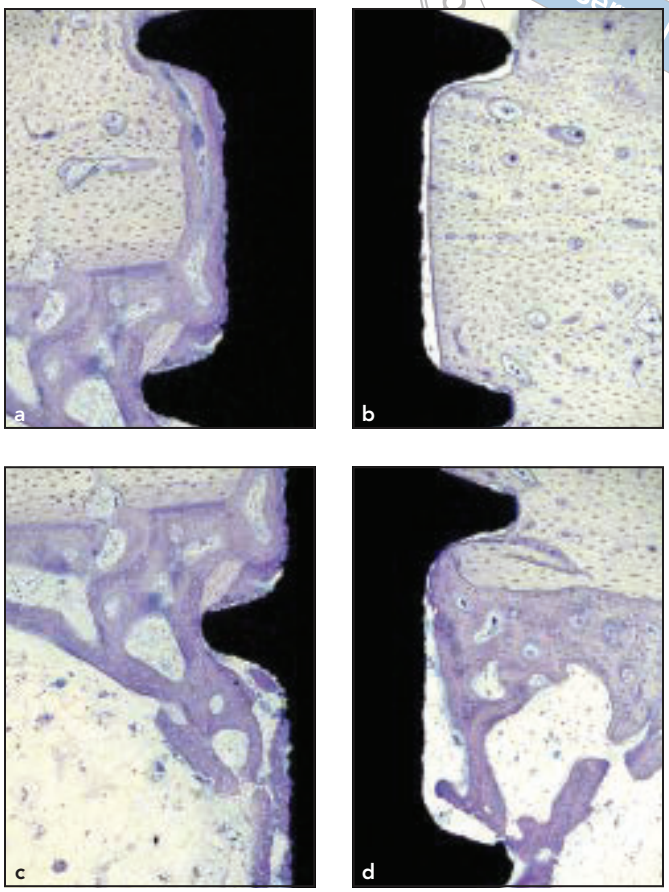

Fig 7 *Light microscopy observations of the undecalcified cut and ground sections after RTQ testing (360 degrees of counter rotation) demonstrated enhanced endosteal bone formation* (a and b) *and endosteal downgrowth* (c and d) *for the test group. Interestingly, the test surface* (a and c) *commonly showed an intact de novo bone-to-implant interface compared with the control* (b and d)*, indicating that the two surfaces had different RTQ failure modes. The test group's interfacial bond appeared robust enough to transition the RTQ fracture away from the surface into the bone, while the control group demonstrated more typical shearing at the interface (scale bar = 800 µm, corresponding to a thread pitch length).*

However, both implant groups showed highly statistically significant increases of their ISQ values after a healing time of 3 weeks ($P \leq .001$).

RTQ measurements

At 3 weeks of follow-up, the test group demonstrated a highly statistically significant increase in mean RTQ value over control implants (32.6 vs 20.6 Ncm, n = 17, $P = .002$) (Fig 6).

Histologic observations and new bone formation around implant surfaces

The light microscope observations of the undecalcified cut and ground sections after RFA and RTQ measurements demonstrated endosteal bone formation (inside the threads against the old cortical bone) and endosteal downgrowth (below the old cortex) in both groups. New bone formation was clearly distinguished from the old bone by demarcation lines. In the test group, more close contact at the interface of the bone and surface was observed compared with the control surface (Fig 7). Since the histologic evaluation occurred after 360 degrees of removal torque, the presence of an intact interface provides evidence of a robust bone-to-implant surface bond. Additional observations also showed more direct contact of bone cells to the implant surface in the test group, potentially signifying enhanced osteoconduction versus the control (Fig 8). At 3-weeks follow-up, post-RTQ, the test group demonstrated a highly statistically significant increase in the mean value of bone formation on the implant surface versus control implants (39.9% vs 29.9%, n = 17, $P = .00021$) (Fig 9).

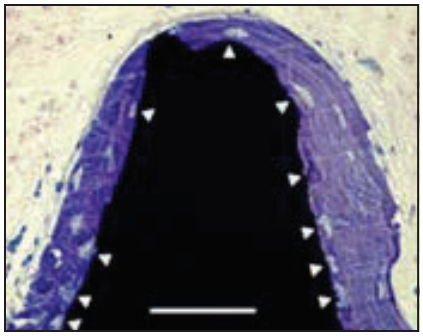

Fig 8 *The test group often presented direct contact of bone cells (arrow heads) to implant surface at 40 × 10 magnification (scale bar = 100 µm) of the undecalcified cut and ground sections.*

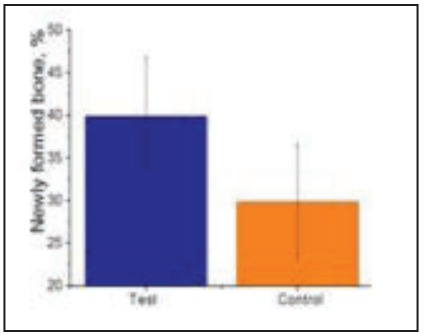

Fig 9 *After RTQ testing, quantification of new bone formation was performed around all inside threads of the implants. The test group demonstrated statistically higher bone formation on the surface compared with the control.*

Discussion

Previous data have shown that the addition of bioactive titanium oxide chemistry (ATiOxB) significantly enhanced osseointegration behavior over microstructured, moderately rough surfaces.[1,3,4,6] The present results are in line with previous findings, with the test and control implants having similar surface roughness and qualitative micron-level topographies but possessing different surface chemistry. These differences resulted in significantly enhanced bone response as compared to the control. Subtle qualitative variations in the submicron topography may also have contributed to a physical interlocking improvement[25]; however, the results can also be explained through the creation of a biochemic bond between the bone and implant interface.[5] In contrast to the TiO_2 chemistry of the control implants, the hydroxyapatite chemistry of the test implants more often resulted in an intact bone-to-implant interface and direct cell contact after RTQ. This observed difference may be the result of a biochemic bond.

In a recent publication, researchers provided further evidence regarding biochemic bonds between the implant surface and newly formed bone tissues.[8] In this preclinical study, smooth implants with near zero micron and nanoscale roughness were used as a constant parameter, with bioactive titanium oxide surface chemistry, ATiOxB, used as the independent variable. The implants with bioactive chemistry demonstrated increases in tensile strength and RTQ indicative of a biochemic bond. Additionally, histologic evaluation showed statistical improvements in bone-to-implant contact, bone area, and mean amount of newly formed bone. The author proposed that the ATiOxB has more electrical and chemical molecular polarity that fractionally charges the surfaces denoted as δ+ and δ−, leading to electrostatic and electrodynamic interactions with the bone healing cascade, eventually concluding with the formation of biochemic bonding at the bone-to-implant interface.

In this study, the micron-scale topographies were held constant and the surface chemistry was modified. The deposition of submicron-scale hydroxyapatite crystals resulted in a surface composed of titanium oxides/hydroxides and calcium phosphate. The resultant surface was similar to those investigated by Jimbo et al in 2012.[26] In that experiment, the researchers investigated differences in biologic response to three different calcium phosphate–based nanostructured surfaces. Atomic force microscopy topographic analysis of test surfaces showed notable differences from the control, but not between the different nanostructured groups. However, the surface chemistries, as determined by x-ray photon spectroscopy, indicated differences in Ca to P ratios for each of the test groups. The biomechanic results demonstrated statistical differences between two of the three test groups versus the control. The authors suggested that the variation in surface chemistries between the three groups accounted for their difference in biologic response versus the control.

The evidence is increasing that the addition of hydroxyapatite, submicron features has an early influence on integration and the biomechanic resistance of titanium

implants to external forces.[18–20,26] The reason for this response remains the subject of considerable academic debate, with data suggesting that both topographic interlocking and biochemic bonding play important roles.

Conclusion

In this 3-week preclinical study, the addition of a discrete crystal deposition of submicron-scale hydroxyapatite on preroughened CP titanium implant surfaces resulted in significantly improved bone response as compared to controls. The test group required higher removal torque values, with its post-torque histology demonstrating both enhanced bone formation and an intact interface indicative of a robust bone-to-implant bond.

Acknowledgment

This project was supported by a grant from Biomet 3i, Palm Beach Gardens, Florida.

References

1. Sul YT, Kang BS, Johansson C, Um HS, Park CJ, Albrektsson T. The roles of surface chemistry and topography in the strength and rate of osseointegration of titanium implants in bone. J Biomed Mater Res A 2009;89:942–950.
2. Sul YT, Johansson CB, Albrektsson T. Oxidized titanium screws coated with calcium ions and their performance in rabbit bone. Int J Oral Maxillofac Implants 2002;17:625–634.
3. Sul YT, Johansson C, Byon E, Albrektsson T. The bone response of oxidized bioactive and non-bioactive titanium implants. Biomaterials 2005;26:6720–6730.
4. Sul YT, Jeong Y, Johansson C, Albrektsson T. Oxidized, bioactive implants are rapidly and strongly integrated in bone. Part 1: Experimental implants. Clin Oral Implants Res 2006;17:521–526.
5. Sul YT. Electrochemical growth behavior, surface properties, and enhanced in vivo bone response of TiO2 nanotubes on microstructured surfaces of blasted, screw-shaped titanium implants. Int J Nanomedicine 2010;5:87–100.
6. Sul YT. The significance of the surface properties of oxidized titanium to the bone response: Special emphasis on potential biochemical bonding of oxidized titanium implant. Biomaterials 2003; 24:3893–3907.
7. Sul YT, Johansson C, Wennerberg A, Cho LR, Chang BS, Albrektsson T. Optimum surface properties of oxidized implants for reinforcement of osseointegration: Surface chemistry, oxide thickness, porosity, roughness, and crystal structure. Int J Oral Maxillofac Implants 2005; 20:349–359.
8. Sul YT, Kwon DH, Kang BS, Oh SJ, Johansson C. Experimental evidence for interfacial biochemical bonding in osseointegrated titanium implants. Clin Oral Implants Res 2013;24(suppl):8–19.
9. Davies JE. Understanding peri-implant endosseous healing. J Dent Educ 2003; 67:932–949.
10. Kikuchi L, Park JY, Victor C, Davies JE. Platelet interactions with calcium-phosphate-coated surfaces. Biomaterials 2005;26:5285–5295.
11. Park JY, Gemmell CH, Davies JE. Platelet interactions with titanium: Modulation of platelet activity by surface topography. Biomaterials 2001;22:2671–2682.
12. Klokkevold PR, Johnson P, Dadgostari S, Caputo A, Davies JE, Nishimura RD. Early endosseous integration enhanced by dual acid etching of titanium: A torque removal study in the rabbit. Clin Oral Implants Res 2001;12:350–357.
13. Baker D, London RM, O'Neal R. Rate of pull-out strength gain of dual-etched titanium implants: A comparative study in rabbits. Int J Oral Maxillofac Implants 1999;14:722–728.
14. Buser D, Nydegger T, Oxland T, et al. Interface shear strength of titanium implants with a sandblasted and acid-etched surface: A biomechanical study in the maxilla of miniature pigs. J Biomed Mater Res 1999;45:75–83.
15. Cordioli G, Majzoub Z, Piattelli A, Scarano A. Removal torque and histomorphometric investigation of 4 different titanium surfaces: An experimental study in the rabbit tibia. Int J Oral Maxillofac Implants 2000;15:668–674.
16. Svanborg LM, Andersson M, Wennerberg A. Surface characterization of commercial oral implants on the nanometer level. J Biomed Mater Res B Appl Biomater 2010;92:462–469.
17. Wennerberg A, Albrektsson T. On implant surfaces: A review of current knowledge and opinions. Int J Oral Maxillofac Implants 2010;25:63–74.
18. Nishimura I, Huang Y, Butz F, Ogawa T, Lin A, Wang CJ. Discrete deposition of hydroxyapatite nanoparticles on a titanium implant with predisposing substrate microtopography accelerated osseointegration. Nanotechnology 2007; 18(24):245101.
19. Mendes VC, Moineddin R, Davies JE. The effect of discrete calcium phosphate nanocrystals on bone bonding to titanium surfaces. Biomaterials 2007;28: 4748–4755.
20. Mendes VC, Moineddin R, Davies JE. Discrete calcium phosphate nanocrystalline deposition enhances osteoconduction on titanium-based implant surfaces. J Biomed Mater Res A 2009;90:577–585.
21. Joy DC. Monte Carlo Modeling for Electron Microscopy and Microanalysis. New York: Oxford University Press, 1995.
22. Donnath K, Breuner G. A method for the study of undecalcified bones and teeth with attached soft tissues. The sage-schliff (sawing aand grinding) technique. J Oral Pathol 1982;11:318–326.
23. Johansson CB. On Tissue Reactions to Metal Implants [thesis]. Gothenburg: University of Gothenburg, 1991.
24. Sul YT, Johansson C, Albrektsson T. Which surface properties enhance bone response to implants? Comparison of oxidized magnesium, TiUnite, and Osseotite implant surfaces. Int J Prosthodont 2006;19:319–328.
25. Davies JE. Bone bonding at natural and biomaterial surfaces. Biomaterials 2007; 28:5058–5067.
26. Jimbo R, Sotres J, Johansson C, Breding K, Currie F, Wennerberg A. The biological response to three different nanostructures applied on smooth implant surfaces. Clin Oral Implants Res 2012; 23:706–712.